

Electronic correlation spectroscopy in condensed matter

B.D. Napitu^{1,2}, Y. Pavlyukh², and J Berakdar²

¹Max-Planck-Institut für Mikrostrukturphysik, Weinberg 1, 06120 Halle, Germany

²Department of Physics, Martin-Luther University, Heinrich-Damerow-Straße 4, 06120 Halle

Abstract. On the basis of formal analysis and the perturbation many-body theory we point out the conditions under which short and long-range electronic correlations in condensed matter can be mapped by means of two-particle coincidence spectroscopy. For particle-impact induced electron emission we show that the coincidence intensity integrated over the slow ejected electron is related to the density-density time correlation function. In the case of a fast incoming and outgoing projectile and a slow emitted electron we relate the intensity to the two-particle and higher order correlations. Effects of two-particle correlations on the two-particle spectral density are investigated by means of the dynamical mean field theory (DMFT) applied to the Hubbard model.

1. Introduction

Under certain conditions the intensity for the simultaneous detection of two high-energy electrons upon the impact of a fast electron can be related to the single-particle spectral density in matter, a fact that has been exploited experimentally to a wide range of materials ([1, 2, 3, 4, 5] and references therein). The general approach as such is known as the $(e, 2e)$ spectroscopy (one electron in, two electrons out) and is being extensively studied in two modes *the transmission* [2] and *the reflection mode* [6, 7]. In the transmission mode an energetic electron beam traverses a free-standing thin film ejecting one electron from the valence-band. The two electrons are detected in the forward direction (with respect to the incoming beam) and the scattering event is justifiably viewed as a direct knock-out of the bound electron. The $(e, 2e)$ is then related to the single-particle spectral density. The low-energy counterpart of these high energy experiments is performed in the reflection mode and has been as well studied both theoretically and experimentally [6, 7, 8, 9, 12, 13, 14]. A variety of materials have been investigated, e.g. insulators [6, 15, 16], clean metals [8, 9, 2, 15], ferromagnets [17] and alloys [18].

The aim of this contribution is to inspect the geometry in which a fast electron losses a small amount of energy and momentum which are still sufficient for the emission of one slow electron from the sample. As shown below depending on the measured cross section one can relate the measured intensity to the density-density correlation function or to the properties of the two-particle spectral function [19]. For the calculations of the latter we start from the Hubbard model and employ the dynamical mean field theory [20, 21]. Calculations of the two-particle spectral function based on the results of quantum Monte-Carlo method [22] for single particle spectral function show that the basic structure is dictated by the local (Hubbard) Coulomb correlation whereas the strength of the peaks in the two-particle spectral functions are determined by the direct two-particle correlations.

2. Low-energy electron emission

We consider the inelastic scattering of incoming electrons with energy $\approx 100\text{eV}$ from a paramagnetic sample. The energy and momentum transfer ω_q and \mathbf{q} to the electronic system is sufficient for the emission of only a slow electron (with few eVs). The $(e, 2e)$ intensity can be expressed in a golden-rule type form as [8, 9, 23] (we operate in units in which $\hbar = 1$)

$$\frac{d\sigma}{d\Omega_q d\omega_q d\Omega_{k_f} d\omega_f} = c' \sum_{\bar{\alpha}_i, \bar{\alpha}_f} p_i |\langle \mathbf{k}' f | W | \mathbf{k}, i \rangle|^2 \delta(\omega_q - \omega_f + \omega_i) \quad (1)$$

$$\approx c \sum_{\bar{\alpha}_i, \bar{\alpha}_f} p_i |\langle f | W(\mathbf{q}) | i \rangle|^2 \delta(\omega_q - \omega_f + \omega_i). \quad (2)$$

Here c' (and c) is a kinematical factor that depends on the flux normalization, Ω_q (Ω_f) is the solid angle characterizing the direction of the momentum transfer (the slow ejected electron), ω_f is the energy of the slow emitted electron. The wave vectors of the incoming and scattered electrons are \mathbf{k} and \mathbf{k}' . $|i\rangle$ and $|f\rangle$ stand for the state vectors of the initial and the final states characterized respectively by a collective set of quantum numbers α_i and α_f and the sum runs over those which are not detected ($\bar{\alpha}_i, \bar{\alpha}_f$). p_i is the statistical weight of the initial state (in the thermodynamic equilibrium $p_i = e^{\beta(\omega_i - \mu)}$ where β is the inverse temperature and μ is the chemical potential). The interaction W of the electron with the target is mediated by an operator that couples to the charge density and $W(\mathbf{q})$ is its Fourier transform over the space of the projectile. Let us inspect the case where the slow electron is not detected or integrated over and (as in most cases) the initial state is not specified. The intensity is then (note $\delta(\omega) = \frac{1}{2\pi} \int_{-\infty}^{\infty} dt e^{i\omega t}$)

$$\frac{d\sigma}{d\Omega_q d\omega_q} = c \sum_{\alpha_i, \alpha_f} p_i \langle i | W^\dagger(\mathbf{q}) | f \rangle \langle f | W(\mathbf{q}) | i \rangle \delta(\omega_q - \omega_f + \omega_i) \quad (3)$$

$$= \frac{c'}{2\pi} \int_{-\infty}^{\infty} dt e^{i\omega_q t} \sum_{\alpha_i} p_i \langle i | e^{iHt} W^\dagger(\mathbf{q}) e^{-iHt} W(\mathbf{q}) | i \rangle \quad (4)$$

$$= \frac{c'}{2\pi} \int_{-\infty}^{\infty} dt e^{i\omega_q t} \langle W^\dagger(\mathbf{q}, t) W(\mathbf{q}, 0) \rangle. \quad (5)$$

From this relation we see that the $(e, 2e)$ intensity is solely determined by the ground-state average of a time correlation of the operator $W(\mathbf{q}, t)$. This results is due to the choice of the experimental conditions, i.e. very asymmetric energies of the electrons. For illustration we note that W we may be written as $W(r) = -\int \frac{\rho(\mathbf{r}')}{|\mathbf{r} - \mathbf{r}'|} d^3\mathbf{r}'$, where $\rho(\mathbf{r}')$ is the charge density. Therefore, eq.(5) reads in this particular case

$$\frac{d\sigma}{d\Omega_q d\omega_q} \propto \tilde{v}(\mathbf{q}) \int_{-\infty}^{\infty} dt e^{i\omega_q t} \langle \rho(-\mathbf{q}, t) \rho(\mathbf{q}, 0) \rangle. \quad (6)$$

where $\tilde{v}(\mathbf{q}) \propto 1/q^2$ is the Fourier transform of the bare interaction and for the Fourier components of the charge density we used the relation $\rho^\dagger(\mathbf{q}, t) = \rho(-\mathbf{q}, t)$. The density-density time correlation function $\langle \rho^\dagger(\mathbf{q}, t) \rho(\mathbf{q}, 0) \rangle$ is derived from a two-particle Green's function $G^{(2)}$ [19] (specifically from the polarization propagator). Under certain conditions specified in [19] one may employ the lowest order of the many-body perturbation expansion of $G^{(2)}$, the so-called random-phase approximation (RPA). Such an approach has recently been implemented numerically for $(e, 2e)$ from clusters and surfaces [24, 25]. An efficient scheme to evaluate $G^{(2)}$ is the topic of current intense research because of its ubiquitous importance for the optical, the electronic and the transport properties of materials. Recently we developed a general method based on the configuration interaction scheme for the calculation of $G^{(2)}$. The results are highly

accurate, however the system size is still limited by computational resources to few hundred atoms [26]. An implementation for (e,2e) reactions is in progress.

From equation (5) we can also infer that the total integrated intensity $\sigma = \int \frac{d\sigma}{d\Omega_q d\omega_q} d\Omega_q d\omega_q$ is dictated by charge-density fluctuations. This statement relies on the structure of the scattering amplitude: While events with large momentum transfer also contribute to the integrated intensity (invalidating thus the relation (5)) the major contributions stem from events with small momentum transfer (note that $\tilde{v}(\mathbf{q}) \propto 1/q^2$), even in the presence of screening (due to the q -dependence of the charge density fluctuations). This has also been observed experimentally [7, 14, 15]. Based on this observation we calculated σ for metallic clusters and fullerene starting from eq.(5) and within the RPA approximation for $G^{(2)}$. Comparison with experiments and with calculations neglecting charge density fluctuations confirmed the decisive role of the collective excitations on the ionisation channel even in these confined systems.

3. The two-particle Green's function

From the preceding arguments we see that the integrated (e, 2e) intensities contain information exclusively related to the sample properties and yield some insight into the influence of the collective modes on single (quasi) particle excitations. For extended systems similar information can be obtained from electron-energy loss spectroscopy [27]. Using spin-polarized electrons [17] allows the investigation of the time-correlation function of the spin density, i.e. the magnetic susceptibility. The fully resolved cross section (2) reveals yet more details on the two-particle (and higher) correlations, not obtainable by single particle spectroscopy, as readily deduced from the relation of the two-particle (screened) interaction $W(q)$ that enters (2) (v is the bare interaction [19, 26]):

$$W = v + vG^{(2)}v, \quad (7)$$

meaning that

$$\begin{aligned} \frac{d\sigma}{d\Omega_q d\omega_q d\Omega_{k_f} d\omega_f} &= c \sum_{\tilde{\alpha}_i, \tilde{\alpha}_f} p_i |\langle f | v(\mathbf{q}) | i \rangle|^2 \delta(\omega_q - \omega_f + \omega_i) \\ &+ c \sum_{\tilde{\alpha}_i, \tilde{\alpha}_f} p_i \left(|\langle f | (vG^{(2)}v)(\mathbf{q}) | i \rangle|^2 + I \right) \delta(\omega_q - \omega_f + \omega_i), \end{aligned} \quad (8)$$

where I is an interference term. The relation (7) is converted into an algebraic equation for W by employing Π_f . The latter is constructed as a product of two dressed single particle Green's functions

$$W = v + v\Pi_f W. \quad (9)$$

At high densities and in the static, long-wave length limit (Thomas-Fermi limit) this integral equation is solvable and one finds out the spatial dependence to be $W_{TF}(r_{ij}) = \frac{e^{-r_{ij}/\lambda_{TF}}}{r_{ij}}$ where λ_{TF} is the screening length (in metals it is on the order of few times the lattice constant). These considerations show that W is short ranged (the case of Coulomb potential and several interesting condensed-matter systems (Wigner crystals, Luttinger liquids ...) are important exemptions). From eqs.(7,9) it follows that $vG^{(2)}v = v\Pi_f W$. The key point now is that the first term in eq.(8) is related to the single particle spectral density of the target $A(\mathbf{q} - \mathbf{k}_f, \omega_q - \omega_f)$ [2] and contains no dynamical dependence on the scattering process (in a one-particle formulation it is the initial-state probability density in momentum-space). Hence this part can be measured or calculated separately and subtracted from the right-hand side of eq.(8). The resulting quantity

we call $\frac{\bar{d}\sigma}{d\Omega_q d\omega_q d\Omega_{k_f} d\omega_f}$, meaning that under the conditions specified above the relation

$$\frac{\bar{d}\sigma}{d\Omega_q d\omega_q d\Omega_{k_f} d\omega_f} = c \sum_{\bar{\alpha}_i, \bar{\alpha}_f} p_i \left(\left| \langle f | (vG^{(2)}v)(\mathbf{q}) | i \rangle \right|^2 + I \right) \delta(\omega_q - \omega_f + \omega_i) \quad (10)$$

applies. Its structure becomes transparent if we adopt a single particle formulation, i.e. if we start from a Bloch initial state $\varphi_{\mathbf{k}}(\mathbf{r}) = u_{\mathbf{k}}(\mathbf{r})e^{i\mathbf{k}\cdot\mathbf{r}}$ with a Bloch wave vector \mathbf{k} and a Bloch amplitude $u_{\mathbf{k}}$. Expanding this state over the reciprocal space with a reciprocal lattice vector \mathbf{G} and expansion coefficients $c_{\mathbf{G}}$ we find

$$u_{\mathbf{k}}(\mathbf{r}) = \sum_{\mathbf{G}} c_{\mathbf{G}}(\mathbf{k}) e^{i\mathbf{G}\cdot\mathbf{r}}, \quad \varphi_{\mathbf{k}}(\mathbf{q} - \mathbf{k}') = \sum_{\mathbf{G}} c_{\mathbf{G}} \delta_{\mathbf{G}+\mathbf{k}, \mathbf{q}-\mathbf{k}'}$$

It is straightforward to show that the interference term I is proportional to $\varphi_{\mathbf{k}}(\mathbf{q} - \mathbf{k}')$, meaning that it is finite only at certain localized regions in momentum space; away from which we access directly $\left| \langle f | (vG^{(2)}v)(\mathbf{q}) | i \rangle \right|^2$ at the energy $\omega_q - \omega_f$.

4. Model calculations for the two-particle Green's function

The central quantity entering equation (10) is $G^{(2)}$. If two electrons are emitted upon a photon absorption the intensity is also related to the two-particle spectral density obtainable from the imaginary part of $G^{(2)}$. Calculations of $G^{(2)}$ are much more involved than those for the single particle Green's function. They are mostly done on the level of model systems. In the framework of a single-band Hubbard model, exact results is obtained for the completely filled band. For arbitrary fillings a number of approximations exist that are based either on the equation of motion approach or on the ladder approximation. e.g., Drchal used the equation of motion to calculate the two-particle spectral density of the valence bands [29]. The single-particle aspects entering in this method are however roughly approximated. Further schemes based on the two particle ladder approximation [30, 31, 32] employ various forms of the single particle Green's function. Treglia *et al.* [31] calculated the one-particle spectrum by employing an (approximate) second order perturbation. Drchal and Kudrnovsky [30] presented a self consistent T-matrix approximation valid for low electron-occupancy only. Seibold *et al.* [33] proposed an approach based on the time-dependent Gutzwiller approximation [34] to calculate the electron-pairing. A common feature of most previous works on the two-particle Green's function is that the single particle parts are treated on a low level of accuracy leading to ambiguity in the interpretation of the results.

In the present work, we start from an accurate description of the single particle aspects accounting fully for electronic correlation (as they enter the Hubbard model) allowing to access the crossover regime from weak to strong coupling. Then the ladder approach for two particle properties is utilized.

4.1. The model Hamiltonian

The single-band Hubbard Hamiltonian reads in standard notation

$$H = \sum_{ij\sigma} t_{ij} c_{i\sigma}^\dagger c_{j\sigma} + U \sum_i n_{i\uparrow} n_{i\downarrow} - \mu \sum_i (n_{i\uparrow} + n_{i\downarrow}) \quad (11)$$

where t , U and μ describe the hopping amplitude, the repulsive on-site Coulomb interaction, and the chemical potential, respectively. The electron interactions influence the single and the two particle properties. On the single particle level electronic correlations are subsumed in a renormalization of the single particle properties, and hence we call this type of effect

indirect correlation whereas, due to the two-particle nature of the Coulomb interaction the two particle or the pair of electrons is directly affected by the Coulomb interaction (and hence we call these type of correlation *direct* correlations). Of course, higher order correlations results in a renormalization of the two-particle features derived with two-particle correlations only. Advances in the theoretical treatments of correlations have been made by inspecting the limit of infinite connectivity $d \rightarrow \infty$ in the Hubbard model [20]. Numerical implementation is accessible upon a mapping of the original problems into the impurity Hamiltonian with an additional self consistency relations [21]. In this approximation known as Dynamical mean field theory (DMFT), local correlation is treated in the mean field level while maintaining temporal fluctuations. The great allure of DMFT lies on its flexibility to be adapted to different systems as long as one can determine the appropriate impurity Hamiltonian of the original problems. Solution of the impurity problems is, however, non-trivial and the most demanding task in the DMFT approach except for some extreme cases or particular Hamiltonian [28]. In this work, DMFT is combined with quantum monte carlo (QMC) [22] to solve Anderson impurity-Hamiltonian applied in the Bethe lattice. The free density of states is given by $D(\epsilon) = \frac{1}{2\pi t^2} \sqrt{4t^2 - \epsilon^2}$. The half bandwidth $D \equiv 2t$ is taken as the energy unit and we focus on the paramagnetic phase. The finite-temperature two-particle Green's function is given as [32]

$$G^{(2)}(\mathbf{q}, \omega) = \int \langle T_\tau c_{\mathbf{k},\sigma}(\tau) c_{\mathbf{q}-\mathbf{k},-\sigma}(\tau) c_{\mathbf{q}-\mathbf{p},\sigma}^\dagger(0) c_{\mathbf{p},-\sigma}^\dagger(0) \rangle \quad (12)$$

with f is a short notation for $-\sum_{\mathbf{k},\sigma} \int_0^\beta d\tau e^{i\omega\tau}$ and $\omega = 2n\pi/\beta$ is the Matsubara frequency. Performing standard S matrix procedure [19] one obtains a set of Feynman diagrams for the two particle Green function. The summation to all orders of the diagrams that represent a direct interaction between single particle dressed Green's function leads to

$$G^{(2)}(\mathbf{q}, \omega) = -\frac{1}{\beta} \sum_{k i \nu} G(\mathbf{k}, i\nu) G(\mathbf{q} - \mathbf{k}, i\omega - i\nu) \Gamma_{\mathbf{kq}}(i\omega) \quad (13)$$

with

$$\Gamma_{\mathbf{kq}}(i\omega) = 1 + \frac{1}{\beta} \sum_{p i \nu'} G(\mathbf{p}, i\nu') G(\mathbf{q} - \mathbf{p}, i\omega - i\nu') \Gamma_{\mathbf{pq}}(i\nu') \quad (14)$$

as the vertex part of particle-particle diagram. Equation (14) can be simplified by exploiting the local nature Coulomb correlation (in the sense of Hubbard) to the form

$$G^{(2)}(\mathbf{q}, \omega) = \frac{\Lambda_{\mathbf{q}}(i\omega)}{1 - U_d \Lambda_{\mathbf{q}}(i\omega)}. \quad (15)$$

U_d denotes the matrix elements connected with the direct Coulomb interaction of the two particles and

$$\Lambda_{\mathbf{q}}(i\omega) = -\frac{1}{\beta} \sum_{\mathbf{p}, i\nu} G(\mathbf{p}, i\nu) G(\mathbf{q} - \mathbf{p}, i\omega - i\nu) \quad (16)$$

is the particle-particle (polarization) Green's function. By using standard analytical continuation and evaluating the imaginary part of the two particle Green's function one arrives at an expression for the two particle spectral function $A^{(2)}(\omega)$. It can be compared with one-photon two-electron emission as follows

$$A^{(2)}(\omega) = \frac{C(\omega)}{1 - U_d C(\omega)}, \quad (17)$$

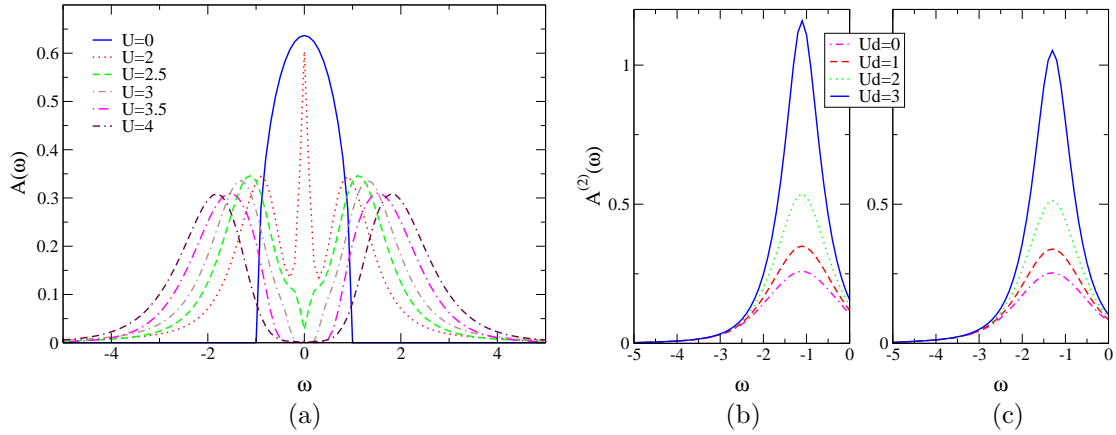


Figure 1. (a) Spectral function of single-particle Hubbard model in the half filled regime ($n = 1$) for various strengths of Coulomb-interaction. Two particle spectral function for $U = 2.5$ (b) and $U = 3$ (c) for various strengths of direct-Coulomb interaction.

where

$$C(\omega) = \int_{-\infty}^{\infty} d\nu \int_{-\infty}^{\infty} d\epsilon f(\nu) [A(\epsilon, \nu + \omega)A(\epsilon, \nu) + A(-\epsilon, \nu - \omega)A(-\epsilon, \nu)], \quad (18)$$

with $f(\nu)$ is the Fermi function and $A(\epsilon, \nu)$ is the single particle spectral function. These results are valid for $\mathbf{q} = 0$.

4.2. Results and discussion

As a pilot calculations we present the spectral function of the single-particle Hubbard model for half filling ($n = 1$) in Fig.1a. As established [28], the finite temperature spectral-function of the Hubbard model in the half filling regime possesses three peaks for moderate Coulomb interactions: two peaks associated with two Hubbard-bands and a quasi-particle peak. The quasi-particle peak gradually disappears with increasing the Coulomb interaction marking the onset of the transition from the metallic to the insulating phase.

The two particle spectral-function can be calculated directly via Equation (17) and Equation (18). As seen from Fig. 1(b,c) the basic structure of the two-particle spectral function is set by the underlying form of the single particle spectral function which in turn depend decisively on U as demonstrated in Fig. 1a. The strength of the peaks in $A^{(2)}$ are strongly dependent on the direct electronic correlations expressed by U_d .

5. SUMMARY

As a summary, we discussed possible information extractable from coincident two electron emission from condensed matter in the case of large energy asymmetry of two outgoing electrons. Depending on the experimental situation one can access information inherent to the two-particle spectral function. For the calculations of this quantity we used the Hubbard model solved numerically using the dynamical mean-field theory within a quantum Monte Carlo implementations. Some pilot results for the two-particle spectral functions are presented and discussed.

6. Acknowledgments

This work is supported by the international Max-Planck research school for science and technology of nanostructures and by the DFG under contract SFB 762.

- [1] R. Camilloni *et al.*, Phys. Rev. Lett. **29**, 618621 (1972)
- [2] E. Weigold and I. E. McCarthy, *Electron Momentum Spectroscopy* (Kluwer Academic/Plenum Publishers, 1999).
- [3] I.E. McCarthy and E.Weigold, Rep. Prog. Phys. **54**, 789879 (1991).
- [4] Zheng *et al.*, Science **270**, 786788 (1995)
- [5] M. A. Coplan, J. H. Moore, and J. P. Doering, Rev. Mod. Phys. **66**, 985 (1994)
- [6] S. Iacobucci, L. Marassi, R. Camilloni, S. Nannarone, and G. Stefani, Phys. Rev. B **51**, 10252 (1995)
- [7] O. M. Artamonov, S. N. Samarin, and J. Kirschner, Applied Physics A **65**, 535 (1997)
- [8] J. Berakdar, S. N. Samarin, R. Herrmann, and J. Kirschner, Phys. Rev. Lett. **81**, 3535 (1998)
- [9] R. Feder, H. Gollisch, D. Meinert, T. Scheunemann, O. M. Artamonov, S. N. Samarin, and J. Kirschner, Phys. Rev. B **58**, 16418 (1998)
- [10] N. Fominykh, J. Berakdar, J. Henk, and P. Bruno, Phys. Rev. Lett. **89**, 086402 (2002).
- [11] J. Berakdar, H. Gollisch, and R. Feder, Solid State Commun. **112**, 587 (1999).
- [12] N. Fominykh, J. Henk, J. Berakdar, P. Bruno, H. Gollisch, and R. Feder, Solid State Commun. **113**, 665 (2000).
- [13] H. Gollisch, N. v. Schwartzberg, and R. Feder, Phys. Rev. B **74**, 075407 (2006).
- [14] S.Samarin *et al.* Surf. Sci. **579**/2-3 166-174 (2005); Phys. Rev. B **72** 235419 (2005); Phys. Rev. Lett, **97** 096402.
- [15] F.O. Schumann, J. Kirschner, and J. Berakdar, Phys. Rev. Lett. **95**, 117601 (2005); F.O. Schumann *et al.*, Phys. Rev. B **73**, 041404(R) (2006); New J. Phys. **9**, 372 (2007); Phys. Rev. B **77**, 235434 (2008)
- [16] N. Fominykh and J. Berakdar, J. of Elec. Spec. and Related Phenomena **161**, 125-127 (2007).
- [17] S.N. Samarin, J. Berakdar, O.M. Artamonov, J. Kirschner, Phys. Rev. Lett. **85**, 1746 (2000); *ibid* J. Berakdar **83**, 5150 (1999); A. Morozov, J. Berakdar, S.N. Samarin, F.U. Hillebrecht, and J. Kirschner, Phys. Rev. B **65**, 104425(2002).
- [18] K. A. Kouzakov *et al.* J. Phys.: Condensed Matter **15**, L41-L47 (2003), Phys. Rev. B **66**, 235114/1-9 (2002)
- [19] A.L. Fetter , J.D. Walecka *Quantum theory of many-particle systems* (McGraw-Hill, 1971).
- [20] W. Metzner and D. Vollhardt Phys.Rev.Lett **62**, 324 (1989).
- [21] A. Georges and G. Kotliar, Phys.Rev.B **45**, 6479 (1992).
- [22] J. Hirsch and R. Fye, Phys. Rev. Lett **56**, 2521 (1986).
- [23] J. Berakdar, M. P. Das, Phys. Rev. A **56**, 1403 (1997)
- [24] O. Kidun, J. Berakdar Phys. Rev. Lett. **87**, 263401 (2001); O. Kidun *et al.* 2002 Surf. Sci. **507** (662); Chem. Phys. Lett. **410** 293 (2005).
- [25] K. A. Kouzakov *et al.* Phys. Rev. A **68**, 022902/1-8 (2003).
- [26] Y. Pavlyukh, J. Berakdar, and W. Hübner Phys. Rev. Lett **100**, 116103 (2008).
- [27] H. Ibach, D.L. Mills, *Electron Energy Loss Spectroscopy and Surface Vibrations.* (New York, Academic Press, 1982).
- [28] A. Georges, G. Kotliar, M. Rozenberg, and W. Krauth, Rev.Mod.Phys **68**, 13 (1996), and references therein.
- [29] V. Drchal, J.Phys.Condens.Matt **1**, 4773 (1989).
- [30] V. Drchal and J. Kudrnovsky, J.Phys.F **14**, 2443 (1984).
- [31] G. Treglia, M. C. Desjonqueres, F. Ducastelle, and F. Spanjaard, J.Phys.C **14**, 4347 (1981).
- [32] W. Nolting, Z.Phys.B **80**, 73 (1990).
- [33] G. Seibold and J. Lorenzana, Phys.Rev.lett **00**, 0000 (2008).
- [34] G. Seibold and J. Lorenzana, Phys.Rev.lett **86**, 2605 (2001).